BUNCH LENGTH BEATING IN PLS STORAGE RING

Yujong Kim*, C. Kim, K. H. Kim, J. S. Yang, M. H. Chun, I. H. Yu
M. Kwon, J. Y. Huang, S. H. Nam, M. H. Cho, W. Namkung, and I. S. Ko
Pohang Accelerator Laboratory, POSTECH, Pohang, 790-784, Korea

Abstract

During the normal operation period in the Pohang Light Source (PLS) storage ring, the spontaneous bunch length oscillation or beating is generated by the nonlinear effects of the RF noise whose frequency is much lower than the bifurcation frequency. Due to the bunch length beating, we can not supply the uniform intensity beams to users. We have described the observed bunch length beating and its mechanism in the PLS storage ring with a simulation.

1 INTRODUCTION

In the Pohang Light Source (PLS) storage ring, we have occasionally met the spontaneous bunch length oscillation or beating during the normal operation period. Although we do not change any machine parameter, this bunch length beating has been spontaneously happened during normal beam operation period. Due to this beating, we can not supply the uniform intensity beams to users. To analyze this phenomenon and solve the problem, we have monitored the beam motion with the streak camera. From its various data, we have found that the bunch length beating has relation with the RF modulation due to a single RF noise whose the amplitude is continuously changed. There are two kinds of the RF modulations to control various beam properties via the longitudinal nonlinear beam dynamics: One is the RF phase modulation, and the other is the RF voltage modulation [1]. Many accelerator laboratories have used the artificial RF phase modulation to control the bunch length, the beam lifetime, and the coupled bunch mode instabilities by injecting a small-amplitude RF signal in the main RF accelerating signal through the RF phase shifter [2], [3]. The natural RF phase modulation can be generated by the RF noises or the RF power supply ripples [3]. Occasionally, there are the RF noise-sidebands around the RF frequency in the No. 3 low level RF system of the PLS storage ring [4]. These are due to a large phase offset at the front of the phase detector in the phase loop of the RF station. On the contrary, in the No. 1 low level RF system, there is occasionally a similar single RF noise whose the frequency is much lower than the synchrotron frequency of 9.773 kHz, and the amplitude is continuously changed. Since the measured bandwidth from the low level RF system to the RF cavity is about 11 kHz, and the bandwidth of RF cavity is about 35.0 kHz, this noise can be transferred to the beams. Therefore, the noise works as the source of the natural RF phase modulation in the PLS storage ring. In this paper, we have described the spontaneous bunch length beating due to a single RF noise via the natural RF phase modulation in the PLS storage ring.

* yjkim@POSTECH.edu

2 RF PHASE MODULATION

2.1 Hamiltonian of RF Phase Modulation

When the beams are under the sinusoidal phase modulation function of $a_m \sin \nu_m \theta_n$, the synchrotron mapping equations for an electron in the phase space coordinates $(\phi,\, \delta)$ can be written as [3]

$$\phi_{n+1} = \phi_n + 2\pi\nu_s\delta_n + 2\pi\nu_m a_m \cos\nu_m\theta_n\,, \quad (1)$$

$$\delta_{n+1} = \delta_n - 2\pi\nu_s \sin\phi_{n+1} - \frac{2\alpha}{f_o}\delta_n\,, \quad (2)$$

where a_m is the modulation amplitude, $\nu_m = f_m/f_o$ is the modulation tune, f_m is the modulation frequency, f_o is the revolution frequency, $\theta_n = 2\pi n$, n is the revolution number, ϕ_n is the synchrotron phase of the electron when the revolution number is n, $\nu_s = f_s/f_o$ is the synchrotron tune, f_s is the synchrotron frequency, $\delta_n = \frac{h\eta}{\nu_s}(\frac{\Delta p}{p})_n$ is the normalized fractional momentum deviation when the revolution number is n, h is the harmonic number, η is the phase slip factor, and α is the synchrotron radiation damping rate. Since the synchrotron radiation damping rate α is much smaller than the synchrotron frequency f_s in the PLS storage ring, the damping term can be ignored from now on. Above mapping equations can be obtained by a Hamiltonian which is given by

$$H = \frac{1}{2}\nu_s\delta^2 + \nu_s\,[1-\cos\phi] + \nu_m a_m \delta \cos\nu_m\theta\,. \quad (3)$$

In order to remove the momentum dependence in the perturbed potential due to the RF phase modulation and to study the parametric resonance, the above Hamiltonian is transformed into new one by a series of the canonical transformations [3]. When the modulation frequency is near an odd multiple of the synchrotron frequency, the parametric resonance can be generated by the RF phase modulation. In this case, the oscillating components of the RF phase modulation are out of phase with the synchrotron oscillations.

When the modulation amplitude is small, the dominant contribution of Hamiltonian comes from the dipole mode parametric resonance term [1]. Near the dipole mode parametric resonance condition, $f_m \simeq f_s$, the time averaged Hamiltonian $\langle H\rangle$ in the resonant rotating frame with the modulation frequency is given by

$$\langle H\rangle = (\nu_s - \nu_m)\tilde{J} - \frac{\nu_s}{16}\tilde{J}^2 - \frac{\nu_s a_m\sqrt{2\tilde{J}}}{2}\cos\tilde{\psi}, \quad (4)$$

where $\tilde{J}$ and $\tilde{\psi}$ are the action-angle coordinates in the resonant rotating frame with the modulation frequency [3]. Their relations with the original coordinates $(\phi,\, \delta)$ can be obtained by a series of the canonical transformations [3]. The first new coordinates $(\tilde{\phi},\, \tilde{\delta})$ have relation with the original ones by the first canonical transformation which is given by

$$\tilde{\phi} = \phi - a_m \sin \nu_m \theta \, , \; \tilde{\delta} = \delta \, . \tag{5}$$

Then, the second new coordinates $(\psi,\, J)$ have relation with the first new ones by the second canonical transformation which is given by

$$\sqrt{2J} \cos \psi = \tilde{\phi} \, , \; \sqrt{2J} \sin \psi = -\tilde{\delta} \, . \tag{6}$$

Note that this canonical transformation is done under the small action limit, i.e., $J \leq 2$ [3]. Finally, the third new coordinates $(\tilde{\psi},\, \tilde{J})$ have relation with the second new coordinates by the third canonical transformation which is given by

$$\tilde{\psi} = \psi - \nu_m \theta - \frac{\pi}{2} \, , \; \tilde{J} = J \, . \tag{7}$$

Since the time averaged Hamiltonian $\langle H \rangle$ is time-invariant in the resonant rotating frame $(\tilde{\psi},\, \tilde{J})$, the electron trajectory is a torus which follows a constant Hamiltonian contour. In the resonant rotating frame, the Hamiltonian equations of motion of Eq. (4) are given by

$$\dot{\tilde{\psi}} = (\nu_s - \nu_m) - \frac{\nu_s}{8} \tilde{J} - \frac{\nu_s a_m}{2\sqrt{2\tilde{J}}} \cos \tilde{\psi} \, , \tag{8}$$

$$\dot{\tilde{J}} = -\frac{1}{2} \nu_s a_m \sqrt{2\tilde{J}} \sin \tilde{\psi} \, . \tag{9}$$

2.2 Stable and Unstable Fixed Points

The stable and unstable fixed points of the time averaged Hamiltonian $\langle H \rangle$, which represent the structure of the resonant islands, can be obtained by putting $\dot{\tilde{\psi}} = \frac{\partial \langle H \rangle}{\partial \tilde{J}} = 0$ and $\dot{\tilde{J}} = -\frac{\partial \langle H \rangle}{\partial \tilde{\psi}} = 0$ [1], [3]. After solving two conditions for the fixed points, we have used a new term $g = \sqrt{2\tilde{J}} \cos \tilde{\psi}$ to represent the phase space coordinate of the fixed points [3]. For $\tilde{\psi} = 0$ or π, the equation for g is given by

$$g^3 - 16 \left(1 - \frac{\nu_m}{\nu_s} \right) g + 8 a_m = 0 \, , \tag{10}$$

[1], [3]. According to the magnitude of the modulation tune ν_m or the modulation frequency f_m, the above cubic equation has different real or complex roots [5].

For $f_m < f_c = \nu_c f_o \equiv f_s \left(1 - \frac{3}{16} (4 a_m)^{2/3} \right)$ which is always less than the synchrotron frequency and is called as the bifurcation frequency, Eq. (10) has an outer stable fixed point A, an inner stable fixed point B, and an unstable fixed point C which are given by

$$A(x) = -8 \sqrt{\frac{x}{3}} \cos \frac{\xi}{3} \, , \tag{11}$$

$$B(x) = 8 \sqrt{\frac{x}{3}} \sin \left(\frac{\pi}{6} - \frac{\xi}{3} \right) \, , \tag{12}$$

$$C(x) = 8 \sqrt{\frac{x}{3}} \sin \left(\frac{\pi}{6} + \frac{\xi}{3} \right) \, , \tag{13}$$

where $x = 1 - \nu_m/\nu_s$, $x_c = 1 - \nu_c/\nu_s$, and $\xi = \arctan \sqrt{(x/x_c)^3 - 1}$. Here, $\tilde{\psi}$ is π for A, and $\tilde{\psi}$ is 0 for B and C [1], [3]. Therefore, electrons will move mostly on the tori with constant Hamiltonians around the two stable fixed points in the phase space. Of course, the electron with the proper Hamiltonian can diffuse from one stable fixed point to the other one through the unstable fixed point C due to mainly the Touschek scattering [2]. When the modulation frequency is much less than the bifurcation frequency, i.e., $f_m \ll f_c$, ξ approaches to $\pi/2$. Therefore, in this limit, $A \to -4\sqrt{x}$, $B \to 0$, and $C \to 4\sqrt{x}$.

When the modulation frequency f_m approaches the bifurcation frequency f_c from below, the outer stable fixed point A and an unstable fixed point C move in, and the inner stable fixed point B moves out. Since $\xi = 0$ at the bifurcation frequency $f_m = f_c$, A is $-(8a_m)^{1/3}$, and both the inner stable fixed point B and the unstable fixed point C are the same as $(4a_m)^{1/3}$.

For $f_m > f_c$, there is only one stable fixed point A which is given by

$$A(x) = -(4a_m)^{1/3} \left\{ \left[\sqrt{1 - (x/x_c)^3} + 1 \right]^{1/3} - \left[\sqrt{1 - (x/x_c)^3} - 1 \right]^{1/3} \right\} .$$

3 SIMULATION AND OBSERVATION

3.1 Simulation Results

We have simulated the RF phase modulation due to the RF noise to analyze the bunch length beating. By solving the time averaged Hamiltonian equations of motion, Eqs. (8) and (9), we can obtain Fig. 1 which shows the 100000 turn tracking results in the resonant rotating frame with the modulation frequency [2]-[4]. Here, all simulation parameters of *may18am*, *may18pm*, and *jun06am* are summarized in Table 1 of the reference [4]. When the modulation frequency is much lower than the bifurcation frequency such as *may18am*, the phase space area, the energy spread, or the bunch length can be increased as the modulation amplitude a_m increases as shown in Fig. 1(a) and (b) [4]. However, at near the dipole mode parametric resonance condition of $f_m = f_c$, the phase space area is reduced and is almost constant though the modulation amplitude is increased as shown in Fig. 1(c) and (d). When the modulation frequency is higher than the bifurcation frequency, there is only one stable fixed point A as shown in Fig. 1(f). All other simulation results are well agreed as described at Section 2.2 and our actual observations [4].

3.2 Observation Results

During the PLS 400 bucket filled normal operation period, we have occasionally met the bunch length beating as

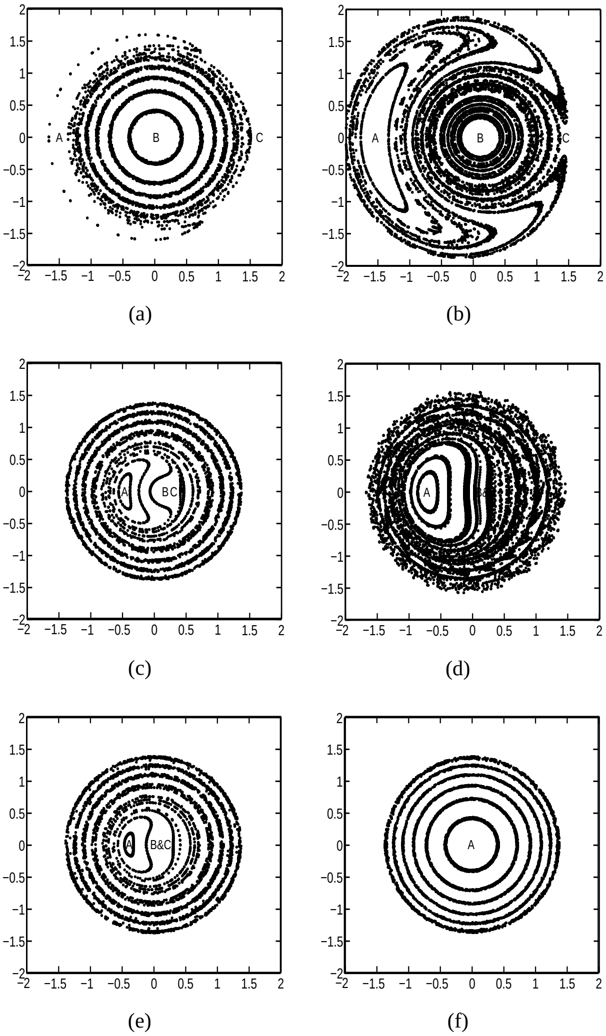

Figure 1: Phase space tracking of the RF phase modulation for (a) $a_m = 0.003$ at *may18am*, (b) $a_m = 0.030$ at *may18am*, (c) $a_m = 0.003$ at *may18pm*, (d) $a_m = 0.030$ at *may18pm*, (e) the bifurcation frequency at *may18pm*, and (f) *jun06am* conditions. Here, the horizontal and the vertical axes mean $\sqrt{2\tilde{J}}\cos(\tilde{\psi} - \nu_m\theta)$ and $\sqrt{2\tilde{J}}\sin(\tilde{\psi} - \nu_m\theta)$, respectively.

shown in Fig. 2 which is observed by the streak camera at 140 mA, 2.5 GeV under a single 5.244 kHz RF noise. Here, the amplitude of the RF noise is continuously changed although its frequency is constant. At first, the most electrons in 400 bunches stay around the inner stable fixed point B when the amplitude of the RF noise is small as shown in Figs. 1(a) and 2(a). As the amplitude of the RF noise increases, some electrons begin to diffuse from the inner stable fixed point B to the outer stable fixed point A via the Touschek scattering as shown in Fig. 2(b) [2]. When the amplitude of the RF noise is high enough, lots of electrons stay around the outer stable fixed point A as shown in Figs. 1(b) and 2(c). Finally, the bunch length is reduced again due to the combined action of the reduced amplitude

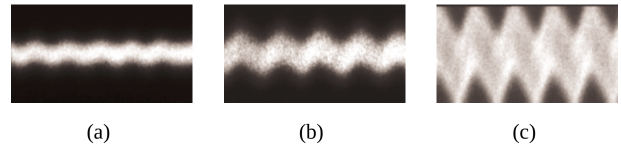

Figure 2: Streak camera images of the beam motion when the bunch length beating is generated due to a single 5.244 kHz RF noise driven phase modulation. The maximum horizontal time scale is 1 ms and the vertical time scale which means the bunch length is same for three cases.

of the RF noise and the synchrotron radiation damping. In this case, almost all electrons return around the inner stable fixed point B again as shown in Fig. 2(a). In this way, the strong bunch length beating is continued until the amplitude of the RF noise is not severely changed any more. The amplitude of the 5.244 kHz noise is changed about 197% during a full cycle of Fig. 2. Although its full cycle period is random due to the randomness of the noise amplitude change, it takes about a few minutes for one full cycle. Note that though the amplitude of the RF noise is high, the strong bunch length beating can not be observed at near the dipole mode parametric resonance condition of $f_m = f_c$ as shown in Fig. 1(d). In this case, only the bunch length compression is observed as described in the reference [4]. Therefore, the bunch length beating can be generated when the modulation frequency is much lower than the bifurcation frequency via the diffusion between two far-off stable fixed points.

4 SUMMARY

We have occasionally observed the bunch length beating when the RF noise frequency is far from the bifurcation frequency. This is due to the RF noise driven phase modulation where the diffusion between two far-off stable fixed points is generated. We have cured this bunch length beating by attaching a mechanical phase shifter in the phase loop of the RF station, and we can supply the uniform intensity beams to users.

5 REFERENCES

[1] S. Y. Lee, *Accelerator Physics*, (World Scientific, Singapore, 1999), p. 243.

[2] J. M. Byrd *et al.*, Phys. Rev. E **57**, 4706 (1998).

[3] H. Huang *et al.*, Phys. Rev. E **48**, 4678 (1993).

[4] Yujong Kim *et al.*, “RF Noise Driven Dipole Mode Parametric Resonance,” these proceedings.

[5] M. R. Spiegel, *Mathematical Handbook of Formulas and Tables*, (McGRAW-HILL, New York, 1985), p. 32.